

# Short electron bunch generation using single-cycle ultrafast electron guns

Arya Fallahi,<sup>1,\*</sup> Moein Fakhari,<sup>1</sup> Alireza Yahaghi,<sup>1</sup> Miguel Arrieta,<sup>1</sup> and Franz X. Kärtner<sup>1,2,3</sup>

<sup>1</sup>Center for Free-Electron Laser Science, DESY, Notkestrasse 85, 22607 Hamburg, Germany

<sup>2</sup>Department of Physics, University of Hamburg, Jungiusstrasse 9, 20355 Hamburg, Germany

<sup>3</sup>The Hamburg Center for Ultrafast Imaging, Luruper Chaussee 149, 22761 Hamburg, Germany

(Received 23 March 2016; published 9 August 2016)

We introduce a solution for producing ultrashort ( $\sim$ fs) high charge ( $\sim$ pC) from ultracompact guns utilizing single-cycle THz pulses. We show that the readily available THz pulses with energies as low as 20  $\mu$ J are sufficient to generate multi-10 keV electron bunches. Moreover, it is demonstrated that THz energies of 2 mJ are sufficient to generate relativistic electron bunches with higher than 2 MeV energy. The high acceleration gradients possible in the structures provide 30 fs electron bunches at 30 keV energy and 45 fs bunches at 2 MeV energy. These structures will underpin future devices for strong field THz physics in general and miniaturized electron guns, in which the high fields combined with the short pulse duration enable electron beams with ultrahigh brightness.

DOI: 10.1103/PhysRevAccelBeams.19.081302

## I. INTRODUCTION

The achievable acceleration gradient in an accelerator device is known to be the main limiting factor governing the emittance and consequently the length of the output bunch. In a conventional particle accelerator, the electrical breakdown of metals introduces a strong limitation on the accelerating fields which are typically 10–100 MV/m [1]. This fact turns out to be the major limit determining the maximum accelerating gradients in many large scale facilities like SLAC [2], CERN's compact linear collider (CLIC) [3] and the design of the next linear collider (NLC) [4]. Moreover, the small acceleration gradient dictates long accelerator lengths, making it the main impediment in developing compact and therefore lower cost devices based on beams of particles with relativistic energies. The desire to realize compact accelerators has spurred much research into the use of alternative acceleration schemes, such as dielectric laser acceleration (DLA) [5–7], laser-driven plasma acceleration (LPA) [8–17], and THz acceleration [18–20].

The empirical studies done by Loew and Wang [1,21] had initially shown that electron field emission, scaling as  $f^{1/2}/\tau^{1/4}$  with  $f$  the operation frequency, and  $\tau$  the pulse duration of the accelerating field, is the main reason for electrical breakdown [22]. The above approximate scaling behavior justified research toward higher operating frequencies and ultrafast schemes to achieve compact accelerators [23]. However, the recent comprehensive study

on breakdown thresholds of various accelerators by Laurent *et al.* [24] and Dolgashev *et al.* [25] demonstrated that pulsed heating of the accelerator walls is the dominant factor limiting acceleration gradients. This conclusion confirmed the observed lower operational gradients in existing facilities when compared with predictions from the previously derived scaling laws. The authors concluded that the pulse duration of the accelerating field plays the major role in the breakdown event, since it is directly linked to the pulse energy governing the pulsed heating in the device. Therefore, focusing efforts on efficient acceleration using short pulses opens new potentials to realize high gradients, which in turn leads to low-emittance bunches and compact devices.

Generally, there is a *conceptual gap* between standard accelerator technology and ultrafast science. Microwave and millimeter-wave technology, used in conventional accelerators, are very well developed for producing continuous wave (CW) radiation. Therefore, accelerators are mostly designed with narrowband excitations. Examples are the widely used cascaded cavities which operate based on a resonant behavior and traveling wave accelerators, in which fields of a guided mode are employed for acceleration [26,27]. Hence, direct usage of a standard accelerator geometry excited by a short pulse laser incurs wasting a large portion of input energy. The goal in this study is to introduce novel structures that aim to accelerate particles from rest using short pulse excitation, which we like to call *single-cycle ultrafast electron guns*.

The last decade has witnessed extensive efforts on acceleration of electrons using optical pulses [5–8,14–17]. However, the acceleration schemes based on optical pulses suffer from the difficulties caused by the short optical wavelengths. Some examples are emittance growth of the electron beam, increased energy spread in the bunch, and challenging timing synchronization for optical acceleration.

\*Corresponding author.  
arya.fallahi@cfel.de

Published by the American Physical Society under the terms of the *Creative Commons Attribution 3.0 License*. Further distribution of this work must maintain attribution to the author(s) and the published article's title, journal citation, and DOI.

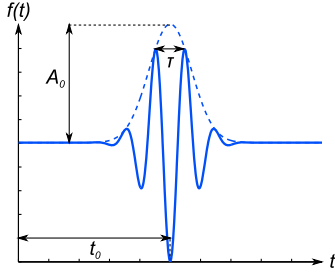


FIG. 1. Temporal signature of a single cycle pulse considered as the excitation in this paper.

Research in THz pulse generation using optical rectification has led to single-cycle pulses [28–30]. The achieved performance in this process has reached percent level optical to THz conversion efficiency [30,31]. Considering that picosecond lasers are necessary for single-cycle THz generation, which have been developed to much higher average power and pulse energies than 100 fs type of lasers, THz acceleration using single-cycle pulses has become a viable option. The first sub-keV devices are already realized and the predictions are evidenced based on experimental results [32]. Nonetheless, this scheme similarly demands broadband devices which function based on short pulse excitations.

This paper presents structures for accelerating particles using single-cycle THz pulses. The considered temporal profile of the excitation is a single-cycle pulse described by  $f(t) = A_0 \exp(-2 \ln 2 (t - t_0)^2 / \tau^2) \cos(\omega(t - t_0) + \phi_0)$ , where  $A_0 = A_0(x)$  and  $t_0 = \pm x/c$  stand for the position dependent amplitude and phase, respectively and  $\phi_0$  is the carrier envelope phase of the signal.  $\omega = 2\pi f_0$  denotes the angular frequency of the signal and  $\tau = 1/f_0$  is the pulse duration of the single-cycle pulse. The temporal signature of such a single-cycle pulse is shown in Fig. 1. Note that the above solution is an approximate solution for a single-cycle pulse and suffers from the inaccuracy of containing a nonzero DC component. However, the error is 0.001 of the peak-field which is not important for the purpose of our study. Although we have considered the illustrated single-cycle pulse, the principle also works for few-cycle pulses, at the expense of additional energy. We present structures which are useful in two different regimes of (i) low energy and (ii) high energy THz beams.

Detailed numerical simulations of the introduced structures play a central role in the presented research. For this purpose, a DGTD/PIC code is employed, which captures all the involved field diffraction effects through the 3D full-vector time-domain solution of the Maxwell's equations using a discontinuous Galerkin time domain (DGTD) method and computes the electron trajectories using a particle in cell (PIC) algorithm. All the bunch evolution calculations in this study are carried out with the consideration of space-charge effects which is simulated using a point-to-point algorithm. For more details on the implemented algorithm, the reader is referred to [33].

For initialization of macro-particles in the guns, we have used the ASTRA photoemission model [34,35]. Note that ASTRA does not simulate the particle acceleration within transient fields and is merely used for bunch generation.

## II. LOW-ENERGY SINGLE-CYCLE ULTRAFAST ELECTRON GUN

### A. Parallel plate gun

Based on the recent demonstration of 1% level optical to THz conversion efficiencies [36], 2-mJ level slightly sub-ps pulses can safely generate 20- $\mu$ J level single-cycle THz pulses typically at 300 GHz central frequency. If this beam is focused down to the diffraction limit, the total electric field at the focus with  $2\lambda$  spot size ( $\lambda$  is the central wavelength) is about 50 MV/m. In this field, initially at rest electrons are able to move maximally  $\delta x = eE\tau/m\omega \approx 7.5 \mu\text{m}$ , being 2–3 orders of magnitude smaller than the wavelength. Consequently, the electrons are affected by both accelerating and decelerating cycles, leading to an inefficient acceleration process. To acquire an efficient acceleration scheme, two goals must be achieved: (1) The accelerating field should be enhanced in order to lengthen the amplitude of electron vibration, and (2) the electron should leave the pulse before the decelerating cycle begins.

Figure 2(a) schematically shows the idea for a two-dimensional (planar) device that pursues the above goals. Two metallic plates form a structure like a 2D horn receiver antenna to focus the incoming linearly polarized THz beam below the diffraction limit. Although the insertion loss of the incident energy is unavoidable, the confined THz beam travels through the region between the two plates and reaches the injection point of electrons. The photocathode laser (usually a UV laser synchronized with the THz pulse) releases an electron bunch from the cathode surface, when the accelerating field of the THz pulse arrives at the injection point. The electrons are then accelerated by the incoming THz beam and leave the acceleration region after a distance  $d$ , i.e., the separation between the two plates. The value of  $d$  is designed so that the electrons experience merely the accelerating half-cycle of the THz pulse. The input THz beam is a 20- $\mu$ J single-cycle Gaussian pulse with central frequency  $f_0 = 300$  GHz and focused to a spot size diameter equal to 2 mm ( $2\lambda$ ). We assume  $L = 500 \mu\text{m}$  and  $D = 50 \mu\text{m}$  and optimize the other dimension for best acceleration, which yields  $\theta = 16^\circ$  and  $d = 30 \mu\text{m}$ . The designed gun realizes a three-fold enhancement in the peak accelerating field ( $E_z^{\text{max}} = 150$  MV/m). Using the PIC simulations, it is demonstrated that an electron released at the instant with acceleration gradient  $E_0 = 50$  MV/m ( $\phi = 20^\circ$ ) gains 1.33 keV energy when leaving the acceleration region. A gun with similar parameters was recently demonstrated with energies up to 0.8 keV [32]. Figures 2(b) and 2(c) show the energy of the electron along its

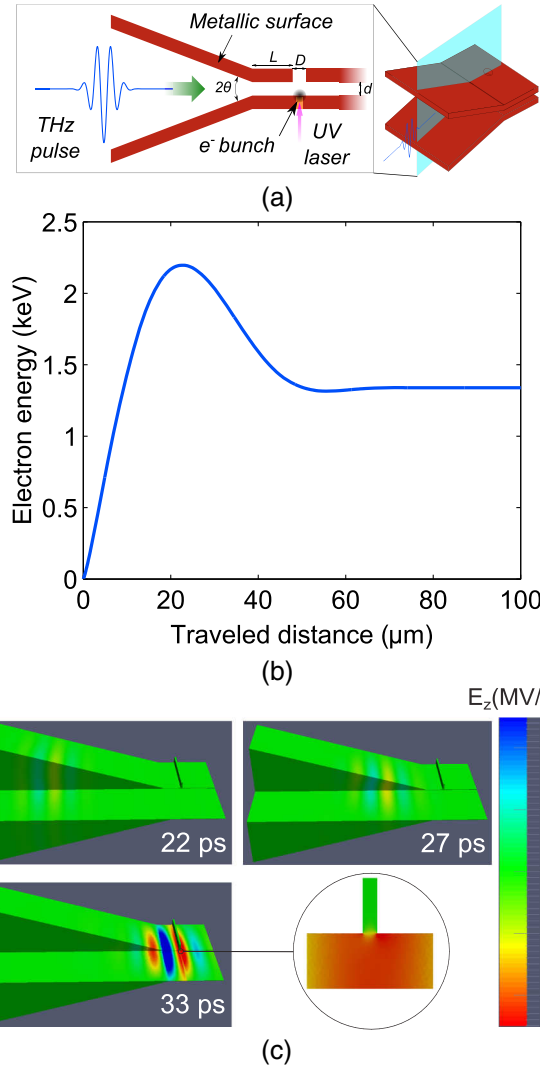


FIG. 2. (a) Schematic illustration of the planar single cycle THz gun, (b) Energy of an electron released at the instant with  $E_z = 50$  MV/m versus the traveled distance, (c) Snapshots of the accelerating field ( $E_z$ ) profile over two half-space cuts of the gun at  $t_1 = 22$  ps,  $t_2 = 27$  ps, and  $t_3 = 33$  ps.

acceleration path as well as the profile of the accelerating field ( $E_z$ ) at three different time points.

### B. Horn gun

There exist several techniques to enhance the efficiency of the above concept in planar devices: (1) In a planar device, the focusing of the THz beam is carried out only in the vertical plane, i.e., the E-plane. The same focusing can also be introduced in the H-plane to further enhance the accelerating field. (2) The focusing in the H-plane introduces cutoff frequencies to the wave propagation. Therefore, the length of the injection region should be reduced to a fraction of the wavelength to enable the *tunneling* of the accelerating field into the acceleration point. (3) Adding a reflector at the receiving side of the

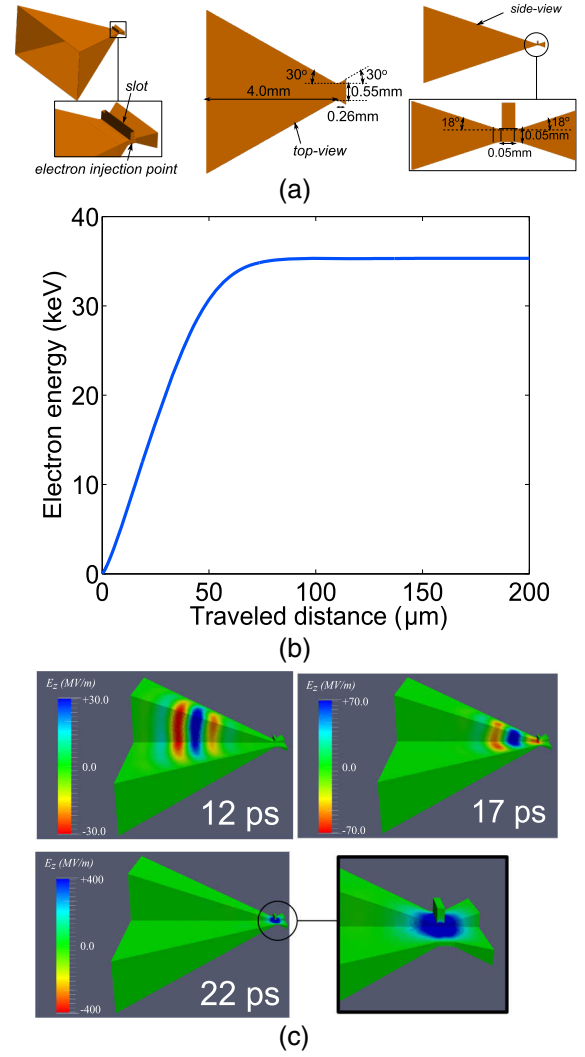


FIG. 3. (a) Schematic illustration of the low energy ultrafast electron gun, (b) Energy of the accelerated electron versus the traveled distance, and (c) Snapshots of ( $E_z$ ) profile over two half-space cuts of the gun. Note the change in the color map scaling for different snapshots.

structure with  $\lambda/4$  distance from the electron injection point, causes the preceding decelerating half cycle to be inverted and added to the accelerating cycle upon reflection. Therefore, the total acceleration gradient at the injection point is enhanced. (4) The same cutoff frequency effect holds also for the receiving side of the structure. Consequently, structuring the right side of the gun similar to the left side enhances the tunneling and thereby increases the acceleration gradient. By taking the above considerations into account, an ultrafast electron gun driven by a low-energy single-cycle THz pulse is designed as shown in Fig. 3(a). The structure consists of two oppositely standing horn couplers (with different lengths) which realize a high acceleration gradient within a single cycle. Thus, the design is named as a *horn gun*. The energy of an electron at rest, injected at the instant with vertical field  $E_z = 50$  MV/m,

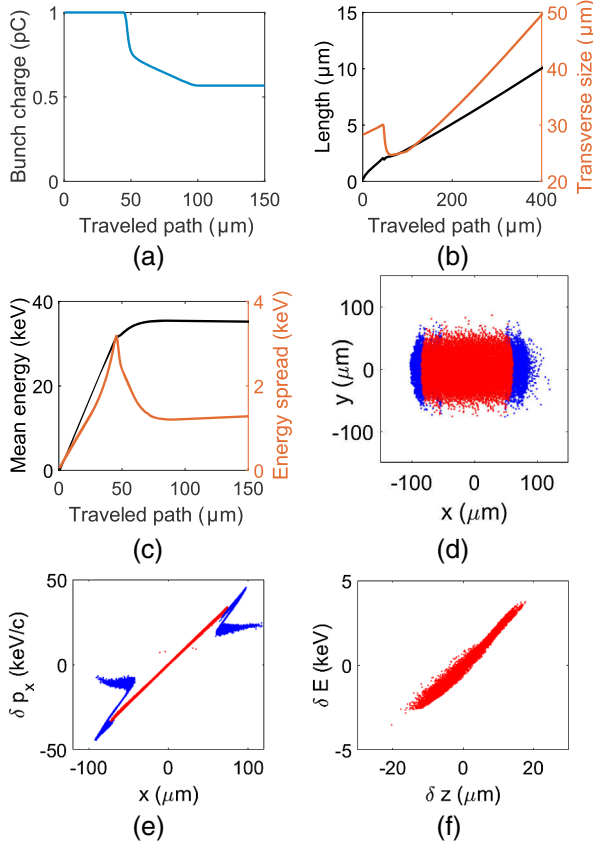


FIG. 4. Acceleration of 1 pC photoemitted bunch in the high energy THz gun: (a) bunch charge, (b) size, and (c) energy in terms of travelled path and (d) shape, (e) transverse phase space, and (f) longitudinal phase-space 100  $\mu\text{m}$  from gun exit are depicted (red dots: output particles; blue dots: trapped particles).

in terms of travel distance as well as snapshots of the accelerating field profile in the device are shown in Figs. 3(b) and 3(c). The simulations evidence an enhancement of the acceleration gradient by a factor of 15, leading to a peak acceleration field of 782 MV/m. The final energy of the electron leaving the gun is 35.3 keV, being ideal for electron diffraction imaging.

For the study of bunch evolution, we assume a copper cathode excited by a UV laser pulse with pulse duration equal to 40 fs and spot size diameter 40  $\mu\text{m}$ . The UV laser energy is chosen such that 1 pC of charge is released which is modeled by 20'000 macro-particles. The evolution of the bunch properties as well as snapshots of the bunch profile are shown in Fig. 4. The mean energy of the bunch increases to 35 keV with an energy spread of about 3%, which happens due to the large spot size of the injected bunch compared to the THz wavelength (1 mm). It is observed that due to the collisions of the electrons with the metallic boundaries due to the transverse momentum of electrons [Fig. 4(e)], only 57% of the photoemitted electrons are extracted out of the gun. This effect shows the limitation on the bunch size and correspondingly the

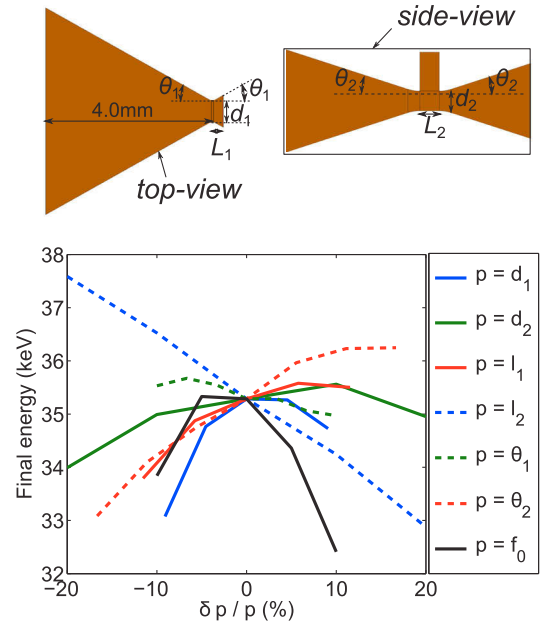


FIG. 5. Results of the sensitivity study for the horn gun. The legend on the left of the plot introduces the studied parameters.

amount of charge which can be accelerated with *good* quality using the proposed THz gun. Our simulations show that placing the introduced gun within a longitudinal magnetic field, i.e. producing the so-called magnetized beam, enhances the aptitude of the gun in terms of accelerated bunch charge. For this purpose, structures producing 1 T-level magnetic fields are required. The final normalized emittances of the bunch are  $(e_{n,x}, e_{n,y}, e_{n,z}) = (0.02, 0.06, 0.013)$  mm mrad and the output bunch length is about 95 fs.

In addition to the bunch acceleration study, a sensitivity analysis of the introduced gun is also of utmost importance. For this purpose, we change each of the values independently by  $\pm 10\%$  from the optimum design, study the THz propagation, inject electrons at the instant when the accelerating field is 50 MV/m, and evaluate the acceleration performance. The results of this analysis evidence maximum 3% change in the final energy as the sensitivity of the device to implementation errors (Fig. 5). This is a very promising sensitivity compared to conventional electron guns, which has its origin in the broadband operation of the device.

### III. HIGH-ENERGY SINGLE-CYCLE ULTRAFAST ELECTRON GUNS

#### A. Two-dimensional concept

In the above designs, it was observed that optimum focusing of the THz beam with only 20  $\mu\text{J}$  energy leads to peak fields as large as 0.8 GV/m on the electron emitter, which is close to the damage threshold of copper and other metals [37]. This means that increasing the energy of the



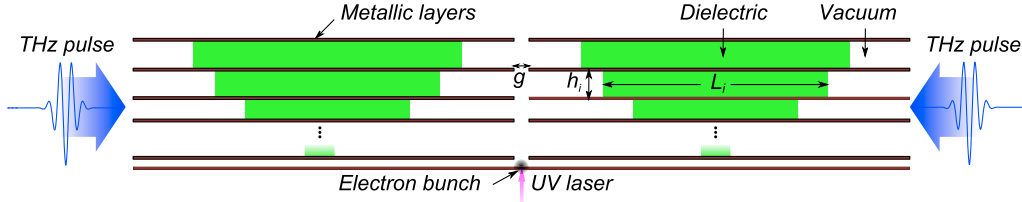


FIG. 6. Schematic illustration of the high-energy ultrafast gun concept.

input THz beam to achieve higher acceleration rates is not realistic. However, today's THz generation technology has realized higher THz energy levels [31]. Consequently, an issue is illuminated; how can one achieve efficient acceleration using high energy short pulses without surpassing the damage threshold? Here, we try to answer this question by introducing structures which operate based on single-cycle THz beams with around 2 mJ energy at 300 GHz central frequency.

For this purpose, two important points must be taken into account: (i) The electron may gain relativistic energy, which intensifies the effect of the transverse magnetic field of the THz pulse. This effect causes a push from the THz pulse along its propagation direction and leads to a curved trajectory for the electron motion. (ii) A high-energy THz beam should not be focused to small spot-sizes to avoid dark current excitation. As a consequence, to achieve an efficient acceleration, matching the phase front of the THz beam with the electron trajectory is essential.

The configuration illustrated in Fig. 6 is a 2D presentation of the concept devised to solve the above two problems. First, two linearly polarized THz beams are symmetrically coupled into the multilayer structure in order to cancel out the magnetic field where they overlap. Second, the phase front of the THz beam is divided into several parts, which are isolated from each other using thin metallic surfaces. In each layer, dielectric inclusions are added to delay the arrival time of the pulse to the acceleration region. By properly designing the filling factor of dielectrics and the thickness of each layer, continuous acceleration of electrons from rest throughout the whole phase front can be achieved.

### B. Multilayer gun

As learned from the study on low energy guns, focusing the incoming excitation in the transverse plane enhances the acceleration efficiency. Furthermore, to avoid suspended thin metallic films in vacuum (Fig. 6), we consider quartz ( $\epsilon_r = 4.41$ ) and teflon ( $\epsilon_r = 2.13$ ) for delaying the arrival time. The structure shown in Fig. 7(a) is the ultrafast THz gun designed for operation based on two single-cycle THz Gaussian beams with each 1.1 mJ energy and central frequency 300 GHz. Without loss of generality, the beam profile is flat top along the acceleration axis and Gaussian in the transverse direction with 2 mm spot size. For a completely Gaussian beam, individual couplers should be

designed to couple the beam energy into the gun input (see Supplementary Material [38]). We assume that two linearly polarized plane waves with the aforementioned temporal signature and peak field 0.5 GV/m illuminate the multilayer gun from both sides. An eight layer configuration is designed for the considered excitation with the thickness of each layer  $h_i = \{0.1, 0.27, 0.35, 0.40, 0.42, 0.43, 0.44, 0.45\}$  mm, and the length of the quartz inclusions  $L_i = \{0.2, 0.865, 1.55, 2.25, 2.95, 3.7, 4.4, 5.1\}$  mm. The size of the acceleration channel is considered to be

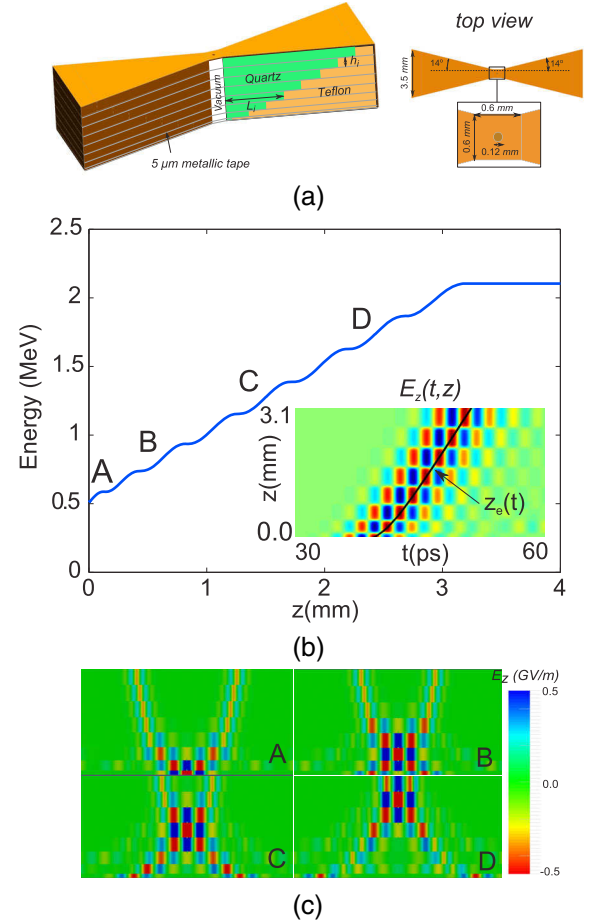


FIG. 7. (a) Schematic illustration of the optimized ultrafast electron gun, (b) electron energy  $E_e(z)$  versus the traveled distance and position of the electron superposed on the accelerating field map  $E_z(z, t)$  as the subset, and (c) snapshots of the field profile at four different instants labeled in (b).

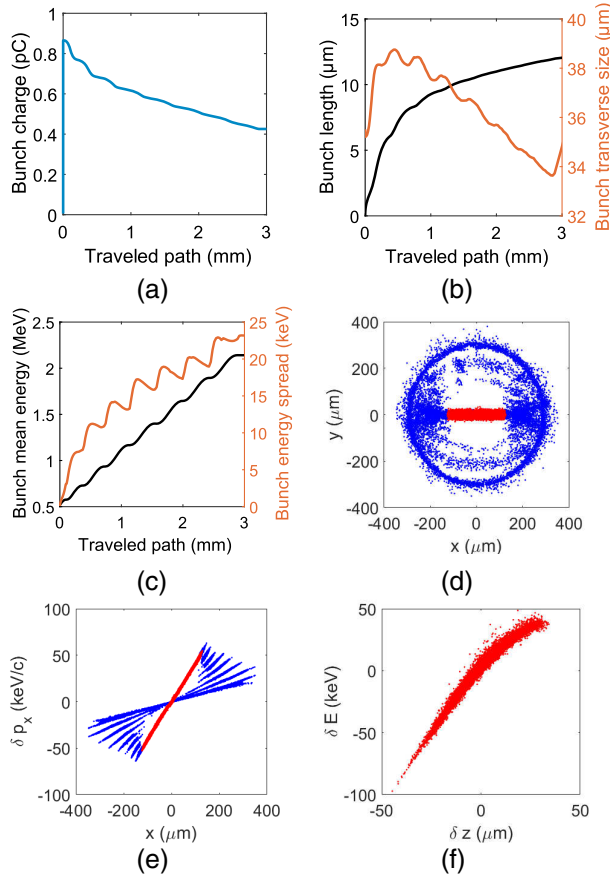


FIG. 8. Acceleration of 1 pC photoemitted bunch in the high energy THz gun: (a) bunch charge, (b) size, and (c) energy in terms of traveled path and (d) shape, (e) transverse phase space, and (f) longitudinal phase-space 3 mm from gun exit are depicted (red dots: output particles; blue dots: trapped particles).

$g = 120 \mu\text{m}$ . The simulation results shown in Fig. 7(b) demonstrate acceleration of an electron from rest to 2.1 MeV. Similar to the previous cases, the electron is released at the point with  $E_z = 50 \text{ MV/m}$ . The realization of phase front matching with the electron motion is shown by snapshots of the field profile in Fig. 7(c) and the subfigure in Fig. 7(b) showing the accelerating field  $E_z(t, z)$  superposed on the particle position  $z_e(t)$ . The small average momentum of the particles in the bottom layers causes small traveling distances within one half-cycle. Therefore, the thicknesses of the layers need to be smaller than the top layers to achieve the required synchronism. This effect leads to the observed gradual increase in the energy gain in different layers [Fig. 7(b)].

By again initializing a photoemitted electron bunch, the bunch evolution in the proposed gun is simulated. We assume that a 40 fs UV laser pulse generates 1 pC charge over a  $60 \mu\text{m}$  spot size, which is modeled using 20'000 macro-particles. The simulation results (Fig. 8) demonstrate acceleration of 40% of the bunch to 2.1 MeV with 1.1% energy spread, output bunch length of 45 fs, and

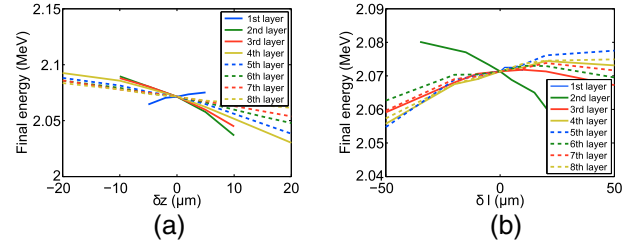


FIG. 9. Sensitivity of the multilayer gun to variations in (a) layer thicknesses and (b) length of quartz inclusions.

normalized emittances equal to  $(e_{n,x}, e_{n,y}, e_{n,z}) = (0.13, 0.13, 0.09) \text{ mm mrad}$ . The main reason for the particle loss is the deflection of the electron trajectories out of the vertical path considered for acceleration. This leads to collision with the metallic layers and in turn loss of electrons, which could again be mitigated by focusing coils (see the Supplementary Material [38]).

Our detailed investigations of the introduced high energy ultrafast gun showed several advantages of such a scheme compared to conventional cascaded or traveling wave cavities. First, due to the inherent operation of the device with broadband excitations, the sensitivity of the gun outcome to the design parameters is minimal. This is illustrated in Fig. 9 for the variations in dielectric lengths and layer thicknesses. It is observed that even 10% change in the designed parameter is tolerated by the device. Second, the pulse heating due to the magnetic field is not only minimized by the single cycle operation, but also the magnetic field is canceled at the electron acceleration region.

#### IV. CONCLUSION

We have presented various structures that can serve as miniaturized electron guns excited by single-cycle THz pulses. Devices for both low energy ( $\mu\text{J}$  level) and high energy (mJ level) THz pulses are proposed. The maximum normal electric field on the surface was allowed to be as high as  $0.8 \text{ GV/m}$ , although the scaling equations predict much higher thresholds for extremely short pulse excitations. This leads to potential additional improvements in terms of acceleration gradient and justifies the use of ultrafast structures to achieve compact accelerators. The presented ultrafast electron guns are promising devices to realize short bunches for applications in electron diffractive imaging, microscopy and compact radiation sources.

#### ACKNOWLEDGMENTS

This work was supported by the European Research Council under the European Union's Seventh Framework Programme (FP/2007-2013)/ERC Grant Agreement No. 609920, the Center for Free-Electron Laser Science at DESY and the excellence cluster The Hamburg Centre for Ultrafast Imaging-Structure, Dynamics and Control of

Matter at the Atomic Scale of the Deutsche Forschungsgemeinschaft. A. Y. is acknowledging support by a George-Foster research fellowship from Alexander von Humboldt foundation.

- [1] G. A. Loew and J. Wang, RF breakdown studies in room temperature electron linac structures, Stanford Linear Accelerator Center, Stanford University, 1988 (unpublished).
- [2] J. Wang and G. Loew, Measurements of ultimate Accelerating Gradients in the SLAC Disk-loaded Structure, Stanford Linear Accelerator Center, Stanford University, 1985 (unpublished).
- [3] L. Linssen, A. Miyamoto, M. Stanitzki, and H. Weerts, [arXiv:1202.5940](#).
- [4] N. Phinney, Next Linear Collider Design Status, Stanford Linear Accelerator Center, Menlo Park, CA, 2002 (unpublished).
- [5] E. Peralta, K. Soong, R. England, E. Colby, Z. Wu, B. Montazeri, C. McGuinness, J. McNeur, K. Leedle, D. Walz *et al.*, Demonstration of electron acceleration in a laser-driven dielectric microstructure, *Nature (London)* **503**, 91 (2013).
- [6] R. J. England, R. J. Noble, K. Bane, D. H. Dowell, C.-K. Ng, J. E. Spencer, S. Tantawi, Z. Wu, R. L. Byer, E. Peralta *et al.*, Dielectric laser accelerators, *Rev. Mod. Phys.* **86**, 1337 (2014).
- [7] J. Breuer and P. Hommelhoff, Laser-Based Acceleration of Nonrelativistic Electrons at a Dielectric Structure, *Phys. Rev. Lett.* **111**, 134803 (2013).
- [8] T. Tajima and J. M. Dawson, Laser Electron Accelerator, *Phys. Rev. Lett.* **43**, 267 (1979).
- [9] G. Malka, E. Lefebvre, and J. L. Miquel, Experimental Observation of Electrons Accelerated in Vacuum to Relativistic Energies by a High-Intensity Laser, *Phys. Rev. Lett.* **78**, 3314 (1997).
- [10] V. Malka, S. Fritzler, E. Lefebvre, M.-M. Aleonard, F. Burgy, J.-P. Chambaret, J.-F. Chemin, K. Krushelnick, G. Malka, S. Mangles *et al.*, Electron acceleration by a wake field forced by an intense ultrashort laser pulse *Science* **298**, 1596 (2002).
- [11] C. Geddes, C. Toth, J. Van Tilborg, E. Esarey, C. Schroeder, D. Bruhwiler, C. Nieter, J. Cary, and W. Leemans, High-quality electron beams from a laser wake-field accelerator using plasma-channel guiding, *Nature (London)* **431**, 538 (2004).
- [12] S. Mangles, C. Murphy, Z. Najmudin, A. Thomas, J. Collier, A. Dangor, E. Divall, P. Foster, J. Gallacher, C. Hooker *et al.*, Monoenergetic beams of relativistic electrons from intense laser-plasma interactions, *Nature (London)* **431**, 535 (2004).
- [13] J. Faure, Y. Glinec, A. Pukhov, S. Kiselev, S. Gordienko, E. Lefebvre, J.-P. Rousseau, F. Burgy, and V. Malka, A laser-plasma accelerator producing monoenergetic electron beams, *Nature (London)* **431**, 541 (2004).
- [14] W. Leemans, B. Nagler, A. Gonsalves, C. Toth, K. Nakamura, C. Geddes, E. Esarey, C. Schroeder, and S. Hooker, GeV electron beams from a centimetre-scale accelerator, *Nat. Phys.* **2**, 696 (2006).
- [15] X. Wang, R. Zgadzaj, N. Fazel, Z. Li, S. A. Yi, X. Zhang, W. Henderson, Y.-Y. Chang, R. Korzekwa, H.-E. Tsai *et al.*, Quasi-monoenergetic laser-plasma acceleration of electrons to 2 GeV, *Nat. Commun.* **4** 1988 (2013).
- [16] W. Leemans, A. Gonsalves, H.-S. Mao, K. Nakamura, C. Benedetti, C. Schroeder, C. Tóth, J. Daniels, D. Mittelberger, S. Bulanov *et al.*, Multi-GeV Electron Beams from Capillary-Discharge-Guided Subpetawatt Laser Pulses in the Self-Trapping Regime, *Phys. Rev. Lett.* **113**, 245002 (2014).
- [17] S. Steinke, J. Van Tilborg, C. Benedetti, C. Geddes, C. Schroeder, J. Daniels, K. Swanson, A. Gonsalves, K. Nakamura, N. Matlis *et al.*, Multistage coupling of independent laser-plasma accelerators, *Nature (London)* **530**, 190 (2016).
- [18] E. Nanni, W. Huang, K. Hong, K. Ravi, A. Fallahi, G. Moriena, R. Miller, and F. Kärtner, Terahertz-driven linear electron acceleration, *Nat. Commun.* **6**, 8486 (2015).
- [19] L. J. Wong, A. Fallahi, and F. X. Kärtner, Compact electron acceleration and bunch compression in THz waveguides, *Opt. Express* **21**, 9792 (2013).
- [20] R. Yoder and J. Rosenzweig, Side-coupled slab-symmetric structure for high-gradient acceleration using terahertz power, *Phys. Rev. ST Accel. Beams* **8**, 111301 (2005).
- [21] J. Wang and G. Loew, in *Proceedings of the 1989 Particle Accelerator Conference, Chicago, IL* (IEEE, New York, 1989), p. 1137.
- [22] W. Kilpatrick, Criterion for vacuum sparking designed to include both rf and dc, *Rev. Sci. Instrum.* **28**, 824 (1957).
- [23] H. H. Braun, S. Döbert, I. Wilson, and W. Wuensch, Frequency and Temperature Dependence of Electrical Breakdown at 21, 30, and 39 GHz, *Phys. Rev. Lett.* **90**, 224801 (2003).
- [24] L. Laurent, S. Tantawi, V. Dolgashev, C. Nantista, Y. Higashi, M. Aicheler, S. Heikkinen, and W. Wuensch, Experimental study of rf pulsed heating, *Phys. Rev. ST Accel. Beams* **14**, 041001 (2011).
- [25] V. Dolgashev, S. Tantawi, Y. Higashi, and B. Spataro, Geometric dependence of radio-frequency breakdown in normal conducting accelerating structures, *Appl. Phys. Lett.* **97**, 171501 (2010).
- [26] T. P. Wangler, *RF Linear Accelerators* (John Wiley & Sons, New York, 2008).
- [27] H. Wiedemann, *Particle Accelerator Physics: Volume I and II (study edition)* (Springer, New York, 2013).
- [28] M. C. Hoffmann and J. A. Fülöp, Intense ultrashort terahertz pulses: generation and applications, *J. Phys. D* **44**, 083001 (2011).
- [29] J. A. Fülöp, L. Pálfalvi, M. C. Hoffmann, and J. Hebling, Towards generation of mJ-level ultrashort THz pulses by optical rectification, *Opt. Express* **19**, 15090 (2011).
- [30] S.-W. Huang, E. Granados, W. R. Huang, K.-H. Hong, L. E. Zapata, and F. X. Kärtner, High conversion efficiency, high energy terahertz pulses by optical rectification in cryogenically cooled lithium niobate, *Opt. Lett.* **38**, 796 (2013).
- [31] W. Schneider, A. Ryabov, C. Lombosi, T. Metzger, Z. Major, J. Fülöp, and P. Baum, 800-fs, 330- $\mu$ J pulses from a 100-W regenerative Yb:YAG thin-disk amplifier at 300 kHz and THz generation in LiNbO<sub>3</sub>, *Opt. Lett.* **39**, 6604 (2014).

- [32] W.R. Huang, A. Fallahi, X. Wu, H. Cankaya, A.-L. Calendron, K. Ravi, D. Zhang, E. A. Nanni, K.-H. Hong, and F.X. Kärtner, Terahertz-driven, all-optical electron gun, [arXiv:1605.06667](https://arxiv.org/abs/1605.06667).
- [33] A. Fallahi and F. Kärtner, Field-based DGTD/PIC technique for general and stable simulation of interaction between light and electron bunches, *J. Phys. B* **47**, 234015 (2014).
- [34] K. Flöttmann, Manual, Version 3, 2014 (2011), [http://www.desy.de/~mpyflo/Astra\\_manual/Astra-Manual\\_V3.1.pdf](http://www.desy.de/~mpyflo/Astra_manual/Astra-Manual_V3.1.pdf).
- [35] D. H. Dowell and J. F. Schmerge, Quantum efficiency and thermal emittance of metal photocathodes, *Phys. Rev. ST Accel. Beams* **12**, 074201 (2009).
- [36] S.-W. Huang, G. Cirimi, J. Moses, K.-H. Hong, S. Bhardwaj, J. R. Birge, L.-J. Chen, E. Li, B. J. Eggleton, G. Cerullo *et al.*, High-energy pulse synthesis with sub-cycle waveform control for strong-field physics, *Nat. Photonics* **5**, 475 (2011).
- [37] M. Dal Forno, V. Dolgashev, G. Bowden, C. Clarke, M. Hogan, D. McCormick, A. Novokhatski, B. Spataro, S. Weathersby, and S. G. Tantawi, rf breakdown tests of mm-wave metallic accelerating structures, *Phys. Rev. Accel. Beams* **19**, 011301 (2016).
- [38] See Supplemental Material at <http://link.aps.org/supplemental/10.1103/PhysRevAccelBeams.19.081302>, for description on the comparison of the DGTD Maxwell solver and CST Microwave Studio, coupler design for the ultrafast high-energy gun, bunch dynamics in single-cycle ultrafast electron guns, and magnetized beams out of ultrafast electron guns.